  Bull. Chem. Soc. Jpn., 54, 1523—1530 (1981)

An *Ab Initio* Calculation of the Electronic Structure of the $[Co(CN_6)]^{3-}$ Ion

Mitsuru Sano, Yasuyo Hatano,† Hiroshi Kashiwagi,†† and Hideo Yamatera*

Department of Chemistry, Faculty of Science, Nagoya University, Chikusa-ku, Nagoya 464

† *Nagoya University Computation Center, Nagoya University, Chikusa-ku, Nagoya 464*

†† *Institute for Molecular Science, Myodaiji, Okazaki 444*

(Received August 14, 1980)

Ab initio LCAO MO SCF calculations were carried out on $[Co(CN)_6]^{3-}$. The character of the wave-functions was discussed in terms of the orbital-mixing rule. The radial distribution of electron density obtained from molecular orbital (MO) calculation was compared with that obtained from X-ray experiments. On the ionization from a metal d-orbital, a significant electronic relaxation was shown to occur, which makes Koopmans' theorem invalid. The calculated excitation energies without a configuration interaction showed a qualitative correspondence with the absorption spectrum.

The electronic structure of the hexacyanocobaltate (III) ion, $[Co(CN)_6]^{3-}$, is of interest from both experimental and theoretical points of view, because this ion is the simplest of the typical symmetrical complexes in which the back-donation of electrons from the metal $d\pi$ to the ligand $p\pi$ orbitals possibly takes place.[1] This complex has been the subject of extensive experimental studies in relation to the electronic structures in the ground and excited states; these studies have included studies of the absorption,[2] infrared (IR),[3,4] Raman,[5] photoelectron,[6,7] and NMR[8,9] spectra, and X-ray analysis.[10,11] A comprehensive review of the chemistry of cyano complexes has been published.[12]

Recently, a precise X-ray crystallographic study of hexamminecobalt(III) hexacyanocobaltate(III) has been made by Iwata and Saito,[13] who have shown the deformation of electron density distribution and calculated the electronic charge on the cobalt atom to be 26.8 ± 0.3 for the cyano complex. Previous theoretical calculations were done for the electronic state of this compound by Kida *et al.*[14] and by Alexander and Gray[2] using the Wolfsberg-Helmholz approach. The energy-level scheme for the octahedral cyanide complexes given by the latter authors have shown the following orbital energy sequence:

$$\sigma(CN^-) < \pi(CN^-) < \sigma(CN^-) < d\pi.$$

The cobalt charge was estimated to be $+0.18$ by Kida *et al.* and $+0.41$ by Alexander and Gray. The aim of the present work is to investigate the cobalt-ligand interaction, the mechanism of π back-donation, and the validity of the application of the Hartree-Fock method to transition-metal complexes. Results are reported for the ground, excited, and ionized states of $[Co(CN)_6]^{3-}$.

Computational Method

The present calculation is of the LCAO MO SCF type, using a basis set of Gaussian functions. The basis set for Co was chosen as follows. The primitive GTF (Gaussian-type function) set, [12s, 6p, 4d], which had been optimized for the ^4F state of the neutral Co atom,[15] was modified by replacing the two most diffuse s functions by tighter functions with the exponents of 0.26 and 0.10 and by adding two supplementary p functions with the same exponents. The resulting [12s, 8p, 4d] functions were contracted to [8s, 6p, 2d]. For C and N, [9s, 5p] sets[16] were contracted to [4s, 2p]. Thus, 348 GTF's were contracted to 158 GTO's (Gaussian-type orbitals). The ion was assumed to be octahedral, and the interatomic distances were taken as:[13]

$$Co\text{-}C = 1.894\,\text{Å}, \qquad C\text{-}N = 1.157\,\text{Å}$$

The calculations were carried out by using a program package called JAMOL2 written by Kashiwagi *et al.*[17] In order to make the integral calculations more tractable, an integral approximation scheme based on semi-orthogonalized orbitals[18,19] was utilized; the threshold value for the degree of overlap was set at 0.0007.

Open-shell calculations for the ionized and excited states have been performed in the restricted Hartree-Fock formalism as given by Roothaan.[20] The corresponding vector coupling coefficients for the various states were calculated according to the reference.[21] The electron-density map was prepared by using the program written by Sano and Miyoshi.[22]

Results and Discussion

The results for the orbital energies and populations of the ground state of the $[Co(CN)_6]^{3-}$ ion have been reported in previous papers.[23–25]

The Electron Density Associated with the Ground States of $[Co(CN)_6]^{3-}$ and CN^-. The charge distribution of the cyanide ion will first be discussed in order to give a basis for the discussion of the electronic structure of the complex. The cyanide ion is isoelectronic with N_2 and CO, and the molecular orbitals of CN^- can be expected to be similar to those of CO. The calculated wave-function contours for the valence shell of the CN^- ion are shown in Fig. 1.[26]

The CN^- 3σ MO consists of the nitrogen 2s and carbon 2s orbitals. The high amplitude in the region midway between the atoms is indicative of substantial σ bonding. In the 4σ MO, a node appears near the nitrogen nucleus; this shows that the nitrogen 2p orbital makes a significant contribution. This MO is derived from the nitrogen sp-hybrid orbital mixed with the predominantly 2s orbital of carbon, and it has approximately the character of the nitrogen lone-pair orbital. The 1π MO shows a higher density at the more electronegative nitrogen. The highest occupied MO (HOMO), 5σ, is strongly polarized towards carbon. This MO is mostly a carbon sp-

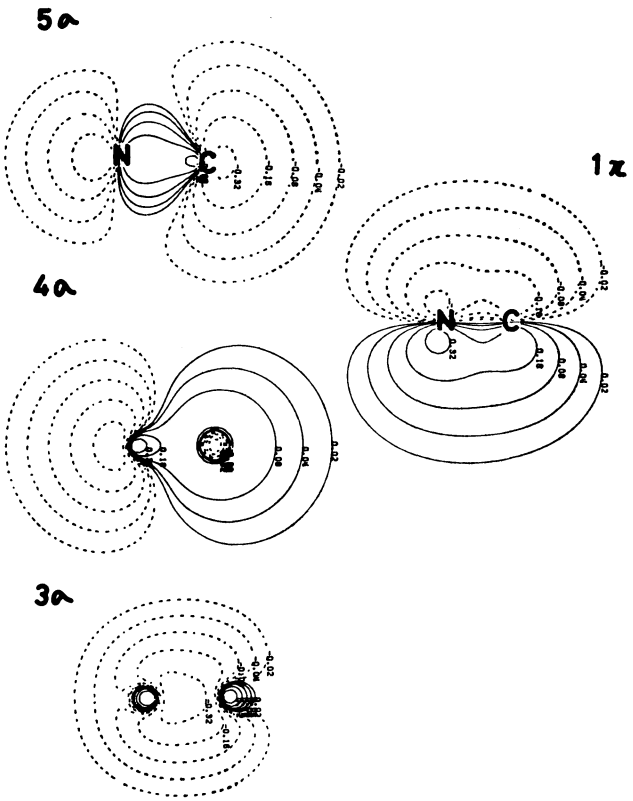

Fig. 1. The wave-function contours for valence shell MO's of the free CN^- ion. The first solid and dotted contours show ± 0.02, respectively, and neighboring contours differ by a factor of two.

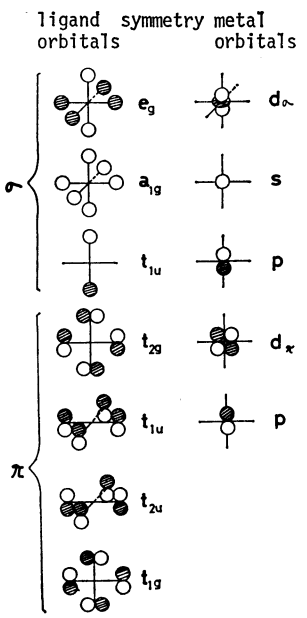

Fig. 2. Octahedral symmetry-adapted combinations of ligand orbitals (left), and the metal-atom orbitals with which they may interact (right). Only one orbital or orbital combination is shown from each degenerate set.

hybrid lone-pair orbital, slightly mixed with the nitrogen p orbital. These MO features explain why the cyanide ion is coordinated to the metal ion not at the nitrogen end, but at the carbon end. The 5σ MO, HOMO of the free CN^- ion, is primarily of the carbon lone-pair, and thus the theory predicts that the coordination of the cyanide ion to the cobalt ion will occur at the carbon end.

The symmetry-allowed interaction between $(CN^-)_6$ and Co^{3+} orbitals in $[Co(CN)_6]^{3-}$ is shown in Fig. 2. Selected wave-function contours for $[Co(CN)_6]^{3-}$ are shown in Fig. 3. In the formation of $[Co(CN)_6]^{3-}$, the σ-type metal 4s (a_{1g}), $3d\sigma$ (e_g), and $4p\sigma$ (t_{1u}) orbitals interact with the CN^- 4σ and 5σ orbitals, while the π-type metal $3d\pi$ (t_{2g}) and $4p\pi$ (t_{1u}) orbitals interact with the CN^- 1π and 2π orbitals. According to the orbital-mixing rule presented by Inagaki *et al.*,[27,28] the interaction of the $|a>$ and $|b>$ orbitals of one system with the $|c>$ orbital of another system will result in a perturbed $|a'>$ orbital consisting of the three orbitals with the signs given in Table 1.

This orbital-mixing rule will now be applied to the interactions between the $Co\sigma$ and the CN^- 4σ and 5σ orbitals and between the $Co\pi$ and the CN^- 1π and 2π orbitals. The σ interaction system will be considered first. The order of orbital energies in the σ system is $4\sigma<5\sigma<Co\sigma$. The new orbital of the lowest energy resulting from the interaction of $Co\sigma$ with 4σ and 5σ is of the $4\sigma+5\sigma+Co\sigma$ type (Case (a)), and the second lowest, of the $5\sigma-4\sigma+$

Table 1. THE ORBITAL MIXING RULE[27,28]

Case	Energy level	Perturbed $\|a'>$ orbital
(a)	$\varepsilon_b>\varepsilon_a$, $\varepsilon_c>\varepsilon_a$	$\|a>+\|b>+\|c>$
(b)	$\varepsilon_b<\varepsilon_a$, $\varepsilon_c>\varepsilon_a$	$\|a>-\|b>+\|c>$
(c)	$\varepsilon_b>\varepsilon_a$, $\varepsilon_c<\varepsilon_a$	$\|a>-\|b>-\|c>$

$Co\sigma$ type (Case (b)). The $7a_{1g}$, $6t_{1u}$, and $4e_g$ MO's correspond to the MO's of the $4\sigma+5\sigma+Co\sigma$ type. The amplitude of the carbon lone-pair increases through the in-phase mixing of 5σ into 4σ, while the amplitude decreases at the nitrogen atom. The ligand parts of $6t_{1u}$ and $4e_g$ are very similar to CN^- 4σ because of the small mixing of CN^- 5σ. In the $7a_{1g}$, however, CN^- 4σ is appreciably modified by CN^- 5σ. The $8a_{1g}$, $5e_g$ and $7t_{1u}$ MO's correspond to the $5\sigma-4\sigma+Co\sigma$ type. This linear combination of 5σ and 4σ with the opposite sign means that the amplitudes are more or less compensated for at the carbon atom and intensified at the nitrogen atom. In the π interaction system, the energies of the orbitals of the t_{2g} symmetry are in the order: $Co\,d\pi < CN^-\,1\pi < CN^-\,2\pi$. The 1π MO is bonding, and the 2π MO is antibonding, with respect to C–N. The $1t_{2g}$ MO consists mainly of Co $d\pi$. The $2t_{2g}$ MO of the $1\pi-2\pi-d\pi$ type results from the 1π ligand orbital through mixing with Co $d\pi$ and 2π orbitals according to the orbital-mixing rule (Case (c) of Table 1). The $2t_{2g}$ MO in Fig. 3 has a node between the cobalt and carbon nuclei. This shows that the $2t_{2g}$ MO consists of a minus combination of $d\pi$ and the dominant CN^- 1π. According to the orbital-mixing rule, the combination of CN^- 2π with $d\pi$ in the $2t_{2g}$ MO is bonding; however, the extent of the mixing of CN^- 2π is small because of its high energy in com-

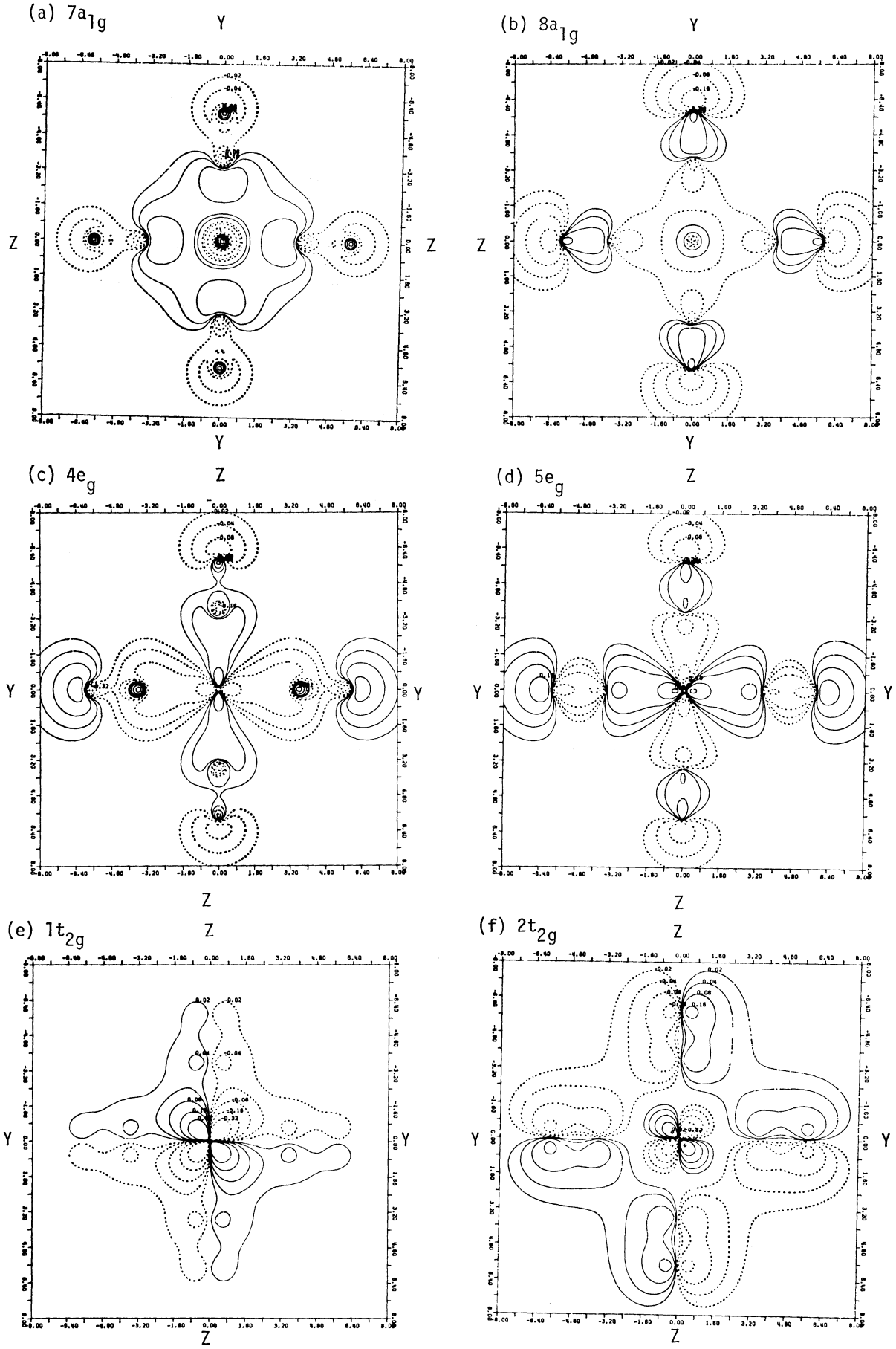

Fig. 3.

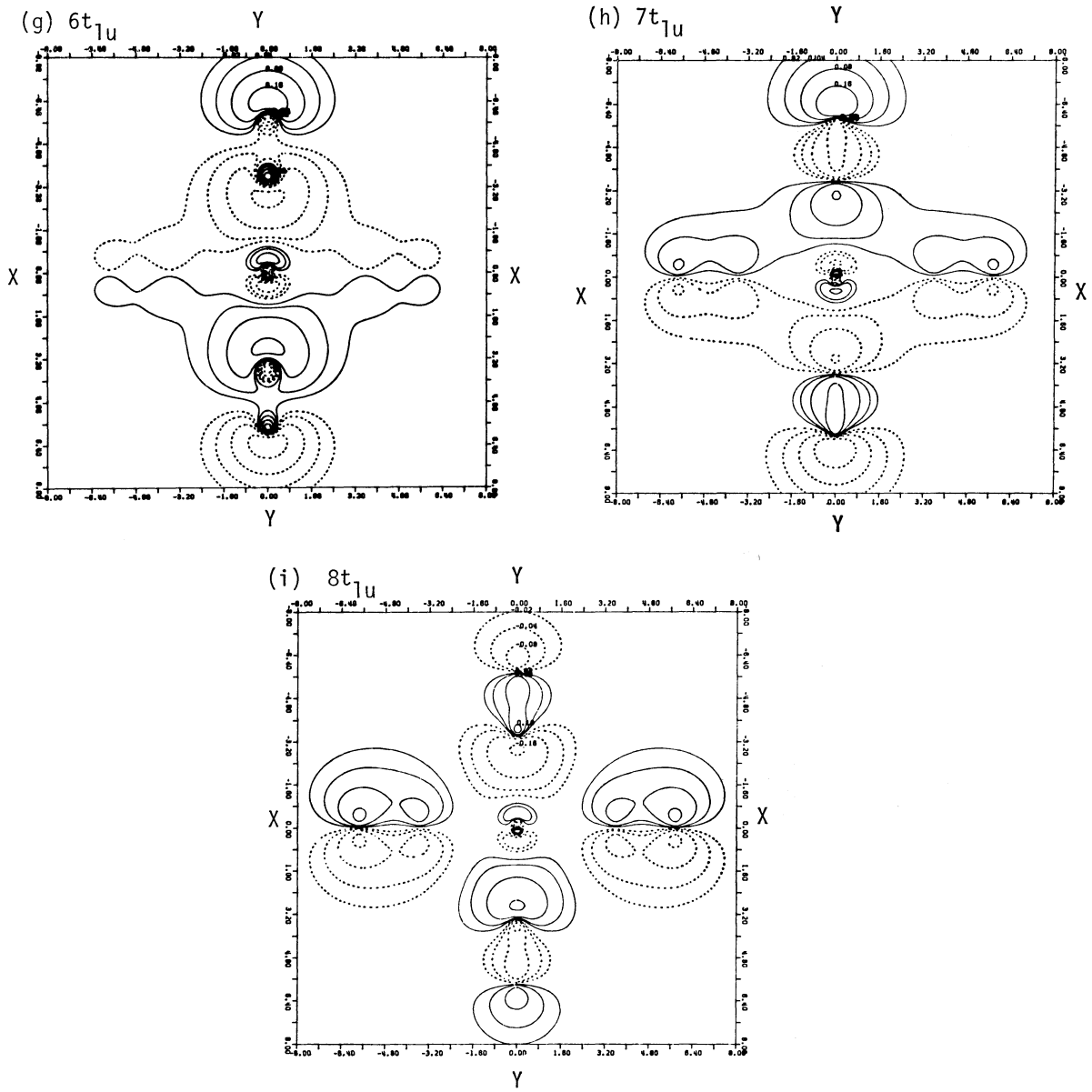

Fig. 3. Selected wave-function contours for valence shell MO's of $[Co(CN)_6]^{3-}$ on the plane containing Co and four CN^-. Each set of contours is drawn in a frame of 16 a.u.×16 a.u. (1 a.u.=0.529 Å= 52.9 pm). The Co atom is located at the center of the frame, and four C and four N atoms at the distances of 3.58 and 5.77 a.u. from the center, respectively. The first solid and dotted contours show ±0.02, respectively, and neighboring contours differ by a factor of two.

parison with CN^- 1π. This interaction scheme of cobalt cyanide is different from that of $d\pi$-π^* assumed by Alexander and Gray.[2] A small contribution of π back-donation still exist in $[Co(CN)_6]^{3-}$.

Figure 4 shows the map of the electron-density difference between $[Co(CN)_6]^{3-}$ and $Co^{3+}(d\pi^6)$ plus six free CN^- ions. The electron density for Co^{3+} was calculated like that of the $t_{2g}{}^6$ electron configuration in octahedral symmetry. The C–N bond length for the free CN^- was assumed to be the same as that in the complex. The CN^- ions were placed along three axes (x, y, z, −x, −y, −z) with the same geometry as in $[Co(CN)_6]^{3-}$. The solid and broken lines denote, respectively, an increase and a decrease in the electron density upon complexation. As can be seen from the increased electron density around the cobalt atom and the decreased density around the ligands, the electron flows from the ligands into cobalt. The positive region corresponding to the cobalt σ orbitals represents an increased electron density attributable to σ donation from the ligands. The decreased electron density in the $d\pi$ orbital indicates π back-donation. The increase in the cobalt charge accompanied by σ donation is larger than the decrease accompanied by π back-donation; thus, the positive charge of the cobalt atom is decreased. The orbital populations ($3d\sigma$, 1.040; 4s, 0.242; 4p, 0.667; and $3d\pi$, 5.885) obtained from the Mulliken population analysis of the semi-double-zeta basis set are consistent with the map. The electron density in the cyanide ligand decreases in the vicinity of the carbon nucleus, increases in the outer region of the carbon atom, and

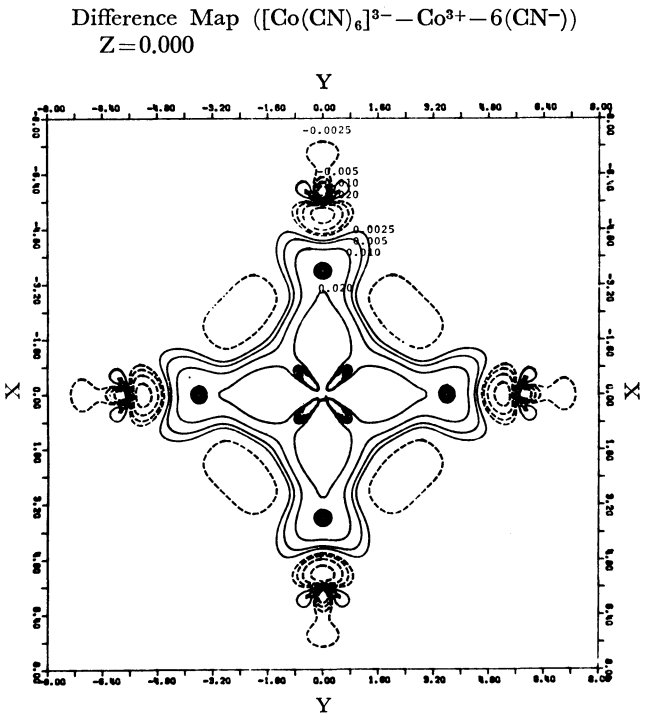

Fig. 4. The electron density difference between $[Co(CN)_6]^{3-}$ and Co^{3+} (with $d\pi^6$ configuration) plus six free CN^- ions. The first solid and dotted contours show ± 0.0025 e(a.u.)$^{-3}$, respectively, and neighboring contours differ by a factor of two.

decreases around the nitrogen nucleus. This shows that the cyanide ion is polarized by the positive charge of cobalt and that, in the carbon atom, the 2s population is decreased and the 2p population is increased. In effect, the nitrogen atom donates an electron density to the cobalt atom through the carbon atom; only slight π back-donation takes place from cobalt to nitrogen.

Comparison with X-Ray Results. In this section, the results of our calculation will be compared with those of the precise X-ray crystallographic study performed by Iwata and Saito,[13] who obtained 26.8 ± 0.3 e as the positive charge on the cobalt atom by directly integrating the electron density of the cobalt atom. They also showed the asphericity of the distribution of Co 3d electrons by difference Fourier synthesis.

The results of the present calculation are shown in Fig. 5, in which the radial distribution of the electron density around the central cobalt nucleus and the integrated number of electrons are plotted against the radius of the sphere, r. It is shown that the calculated radial electron density has a minimum value at 0.95 Å from the cobalt nucleus and that the number of electrons contained in a sphere of the 0.95 Å radius is 24.7. Both of these values are considerably lower than the corresponding experimental values of 1.22 Å and 26.8 ± 0.3. However, the integration of the electron density up to 1.22 Å gives 26.7 electrons, in good agreement with the experimental results. A fine structure which has not been reported by Iwata and Saito is observed: a minimum at 0.3 Å and a

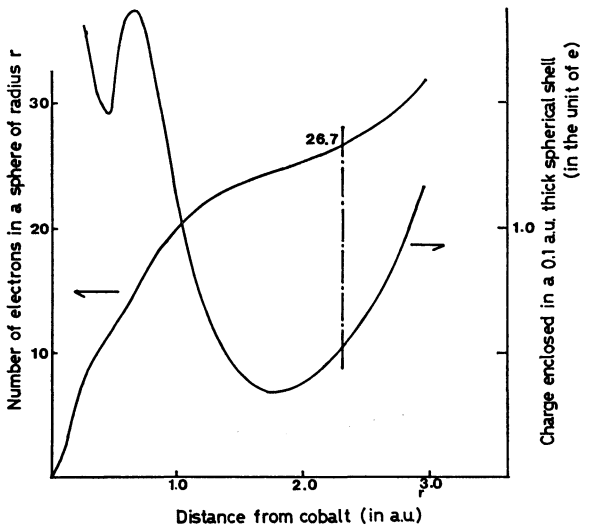

Fig. 5. The radial distribution and integrated number of electrons around the central cobalt atom.

maximum at 0.4 Å from the cobalt nucleus. Thermal vibrations in the experimental system may blur the fine structure and make the effective radii of orbitals greater than those for the frozen system assumed in the calculation.

Orbital Energies and Ionization Potentials. The sequence of orbital energies for the $[Co(CN)_6]^{3-}$ ion has already been reported.[23] The important finding was that the ordering:

$$\sigma(CN^-) < 3d\pi < \sigma(CN^-) < \pi(CN^-)$$

is different from that:

$$\sigma(CN^-) < \pi(CN^-) < 3d\pi$$

which has usually been assumed.

According to Koopmans' theorem,[29] the ionization potential (I.P.) associated with the removal of one electron from a given orbital of a closed-shell system is equal to the corresponding orbital energy with the sign inverted. Veillard and Demuynck[30] reported that Koopmans' theorem is not always valid and that it is not possible to rely on Koopmans' theorem to establish the spectral sequence. The most consistent way to compute ionization potentials is to calculate and compare two total energies at the same level of approximation for the molecule with N electrons and the ion with $N-1$ electrons. This is called the ΔSCF method. The ΔSCF calculation has been carried out in the following way. The energies of the electronic state with a hole in a given orbital and of the ground state are independently calculated in the SCF procedure; then the difference between them gives the ionization potential. The calculation has been carried out for the electronic states resulting from the removal of an electron from the orbitals, $8a_{1g}$, $5e_g$, $1t_{1g}$, $1t_{2g}$, $8t_{1u}$, and $1t_{2u}$. The geometry in these electronic states has been kept the same as that of the N-electron state; hence, the computed ionization energies may be compared with the vertical I.P.

The ΔSCF results are given in Table 2, together with the orbital energies in the ground state, $^1A_{1g}$.

TABLE 2. COMPUTED IONIZATION ENERGIES OF $[Co(CN)_6]^{3-}$

Species	Orbital from which an electron is removed	State	Energy[a]	Computed I.P.[b]	Koopmans' I. P.
$[Co(CN)_6]^{3-}$		$^1A_{1g}$	−1934.402		
$[Co(CN)_6]^{2-}$	$8t_{1u}$	$^2T_{1u}$	−1934.379	0.023	0.029
	$1t_{1g}$	$^2T_{1g}$	−1934.378	0.024	0.035
	$1t_{2u}$	$^2T_{2u}$	−1934.361	0.041	0.052
	$5e_g$	^2E_g	−1934.336	0.066	0.103
	$8a_{1g}$	$^2A_{1g}$	−1934.280	0.122	0.133
	$1t_{2g}$	$^2T_{2g}$	−1934.472	−0.070	0.250

a) Values in a.u. b) I.P. computed as the difference in the energy values for the ionized and ground states. (For the negative value, see the text and Ref. 31.)

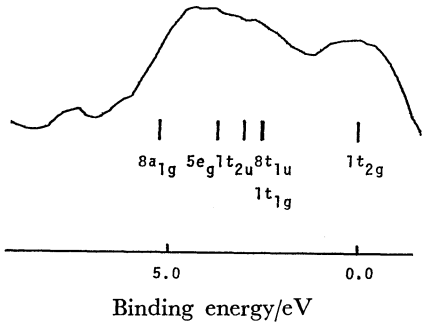

Fig. 6. Valence shell XPS and ΔSCF orbital energies.

The ΔSCF orbital energies decreased in the order:

$$3d\pi(1t_{2g}) > \pi(CN^-) > \sigma(CN^-)$$

which is similar to those in previous reports.[2,14] The computed I.P. corresponding to the removal of one electron from the $1t_{2g}(d\pi)$ orbital is negative; that is, the $[Co(CN)_6]^{2-}$ ion in its $^2T_{2g}$ state is shown to be more stable than the $[Co(CN)_6]^{3-}$ ion in its ground state, $^1A_{1g}$. However, $[Co(CN)_6]^{3-}$ is stable in actual systems, since the trinegative ion is stabilized to a greater extent than the dinegative ions by the electrostatic interaction with surrounding cations.[31] The experimental and calculated ionization potentials are compared in Fig. 6, in which the energy of the $d\pi$ orbital is taken as the reference in the comparison of the calculated I.P. with the X-ray photoelectron spectrum. The computed values show a good correspondence with the spectrum. This may support a previously proposed assignment for the valence-level peaks of XPS.[6,7] Koopmans' theorem may be valid when the electronic relaxation upon ionization and the change in correlation energy between the initial and the ionized states are sufficiently small to be ignored. The following discussion will attempt to clarify the importance of the electronic relaxation upon the ionization of a d-orbital electron. Figure 7 shows a map of the electron-density difference between the $8a_{1g}$ (located dominantly in the ligands) hole state and the $^1A_{1g}$ ground state, while Fig. 8 is a similar difference map for the $1t_{2g}$ (dominantly metal $d\pi$) hole state and the ground state. In these maps, the solid and broken lines denote, respectively, decreased and increased electron density upon ionization. The density map of $8a_{1g}$ MO is shown in Fig. 9; it resembles the difference map for the $8a_{1g}$ hole state (Fig. 7).

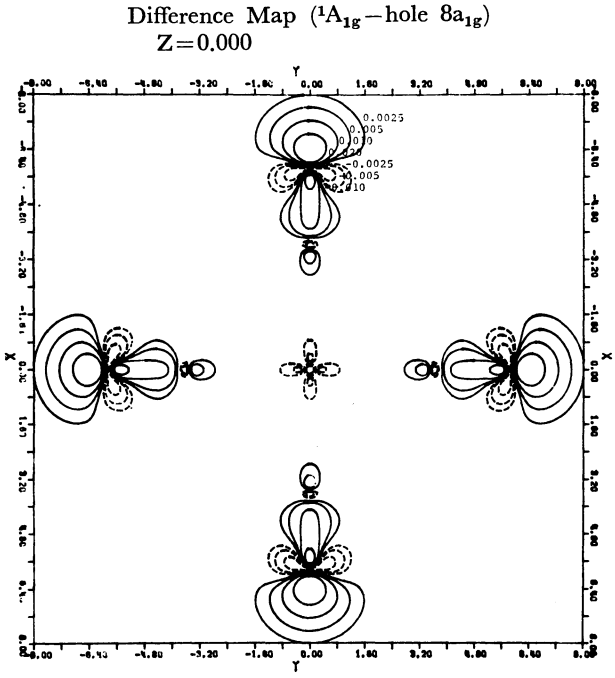

Fig. 7. The electron density difference between the $^1A_{1g}$ ground state and the $8a_{1g}$ hole state. The first contours show ± 0.0025 e(a.u.)$^{-3}$, neighboring contours differing by a factor of two. The positive and negative values represented by the solid and dotted curves correspond to decrease and increase in electron density upon the ionization, respectively.

This means that ionization from the $8a_{1g}$ orbital is accompanied by only a slight relaxation. Thus, Koopmans' theorem is valid for $8a_{1g}$ MO, which is essentially a ligand orbital. The map of the $1t_{2g}$ MO function (Fig. 3-e) is significantly different from the map of the difference between $^1A_{1g}$ and $^2T_{2g}$ states (Fig. 8). The latter shows that a decrease in $3d\pi$ electron density is accompanied by an increase in the $3d\sigma$ density, indicating an extensive relaxation upon ionization. The situation is more clearly demonstrated by Table 3, which shows the orbital population differences between the ground and ionized states on the semi-double-zeta basis set. The positive value shows an increase, and the negative value, a decrease, in the electron population caused by ionization. The Mulliken orbital populations for $8a_{1g}$ and $1t_{2g}$ are also given for the sake of comparison. It should be

TABLE 3. CHANGE IN ORBITAL POPULATION UPON IONIZATION

		$^2A_{1g}-{}^1A_{1g}$ Population change	($8a_{1g}$ MO Population)	$^2T_{2g}-{}^1A_{1g}$ Population change	($1t_{2g}$ MO Population)
Cobalt	3dσ	0.014		0.705	
	3dπ	0.001		−0.920	(0.894)
	4s	−0.020	(0.020)	0.056	
	4p	0.005		0.153	
Atomic charge		0.000		0.007	
Carbon	2s	−0.116	(0.050)	−0.646	
	2pσ	−0.220	(0.127)	−0.340	
	2pπ	−0.074		0.817	(0.092)
Atomic charge		−0.410		−0.169	
Nitrogen	2s	0.028	(0.231)	0.298	
	2pσ	−0.676	(0.572)	−0.217	
	2pπ	0.058		−0.919	(0.014)
Atomic charge		−0.590		−0.838	

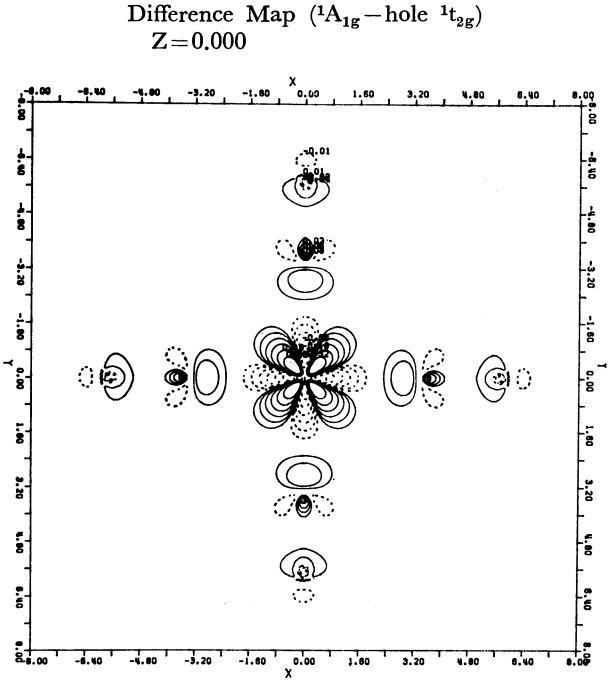

Fig. 8. The electron density difference between the $^1A_{1g}$ ground state and the $1t_{2g}$ hole state. The first contours show ±0.01 e(a.u.)$^{-3}$, neighboring contours differing by a factor of two. See also the caption to Fig. 7.

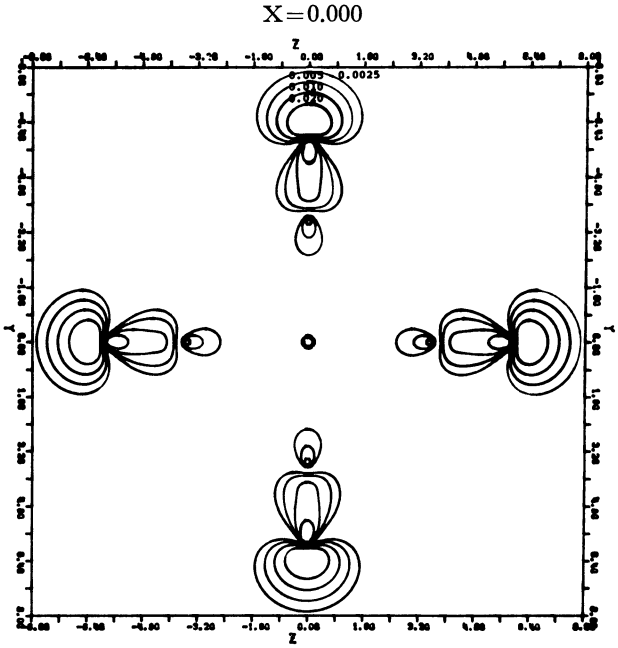

Fig. 9. The electron density map for $8a_{1g}$ MO. The first contour shows 0.0025 e(a.u.)$^{-3}$, neighboring contours differing by a factor of two.

noted that the Co atomic charge is scarcely changed by $8a_{1g}$ ionization or even by the ionization of the $1t_{2g}$ electron, which is dominantly the Co 3dπ electron. The $1t_{2g}$ ionization in effect removes an electron from the nitrogen atoms, not from the cobalt atom. This orbital relaxation explains why the low-lying $1t_{2g}$ electron is most easily ionized and why Koopmans' theorem becomes invalid.

The Excited States of the d-d Transition. In this section we will present some results relative to the excited states resulting from d-d transitions. As found in many other studies of transition metal complexes,[30,32] the excitation energy is not merely the difference between the energies of the occupied and virtual orbitals in the ground state. A rigorous way to calculate the transition energy is to achieve separately energy minimization for the ground and excited states and to equate the difference in their energies with the transition energy, E_{ij}:

$$E_{1j} = E_j - E_1,$$

where the subscripts i and j refer to the ground and excited states respectively. Restricted Hartree-Fock-type calculations have been performed on the two lowest triplet and the two lowest singlet excited states derived from d-d transitions, as is shown in Table 4. All the calculations were performed on the full octahedral space group. The ordering of the excited levels is in good agreement with that predicted by ligand-field theory with empirical parameters.[33] However,

TABLE 4. TOTAL ENERGIES AND RELATIVE ENERGIES OF VARIOUS *d*-STATES

State	Configration	Total energy/a.u.	Relative energy/eV
$^1A_{1g}$	t_{2g}^6	−1934.4016	0.0
$^3T_{1g}$	$t_{2g}^5e_g^1$	−1934.3325	1.88
$^3T_{2g}$	$t_{2g}^5e_g^1$	−1934.2928	2.96
$^1T_{1g}$	$t_{2g}^5e_g^1$	−1934.2745	3.46 (3.97)[a]
$^1T_{2g}$	$t_{2g}^5e_g^1$	−1934.2478	4.19 (4.77)[a]

a) In the parentheses the experimental values are shown.

the energies calculated for the $^1T_{1g}$ and $^1T_{2g}$ states are smaller than the spectroscopic data[2] by about 0.5 eV. Although the Hartree-Foock calculations without configuration interactions gave a qualitative correspondence with the spectrum, a more elaborate treatment is necessary for a quantitative agreement.

Conclusions

The electronic structure of the $[Co(CN)_6]^{3-}$ ion has been investigated by the LCAO MO SCF method, using a double-zeta basis set of Gaussian orbitals. The following results were obtained;

(1) The interaction of cobalt and cyanide ions can be satisfactorily explained in terms of the orbital-mixing rule.

(2) The σ donation from cyanide to cobalt is the dominant interaction, while the π back-donation is weak in $[Co(CN)_6]^{3-}$.

(3) Koopmans' theorem holds approximately for the ligand orbitals, but not for the metal 3d orbitals.

(4) An extensive electronic relaxation occurs during the ionization from a metal d orbital.

(5) The calculated value for the number of electrons around the cobalt atom is in good agreement with the experimental values.

(6) The d-d transition energies obtained by the Hartree-Fock calculation show a qualitative correspondence with the spectrum.

The work was partly supported by the Joint Studies Program (1979—1980) of the Institute for Molecular Science. The computations reported in this paper have been carried out on FACOM 230-75 computers of the Nagoya University Computation Center and the Hokkaido University Computing Center, while the calculation of the electron-density map has been carried out on the HITAC M-180 computer of the Institute for Molecular Science.

References

1) F. A. Cotton and G. Wilkinson, "Advanced Inorganic Chemistry," 3rd ed, John Wiley & Sons, New York (1972), p. 605.

2) J. J. Alexander and H. B. Gray, *J. Am. Chem. Soc.*, **90**, 4260 (1968).

3) K. Nakamoto, "Infrared and Raman Spectra of Inorganic and Coordination Compounds," 3rd ed, John Wiley & Sons, New York (1978).

4) L. H. Jones and B. I. Swanson, *Acc. Chem. Res.*, **9**, 128 (1976).

5) W. P. Griffith and G. T. Turner, *J. Chem. Soc.*, **1970**, 858.

6) A. Calabrese and R. G. Hayes, *J. Am. Chem. Soc.*, **96**, 5054 (1974).

7) N. G. Vannerberg, *Chem. Scripta*, **9**, 122 (1976).

8) M. Hirota, Y. Koike, H. Ishizuka, A. Yamasaki, and S. Fujiwara, *Chem. Lett.*, **1973**, 853.

9) J. J. Pesek and W. R. Mason, *Inorg. Chem.*, **18**, 924 (1979).

10) R. R. Ryan and B. I. Swanson, *Inorg. Chem.*, **13**, 1681 (1974).

11) S. Jagner, *Acta Chem. Scand.*, **A29**, 255 (1975).

12) A. G. Sharpe, "The Chemistry of Cyano Complexes of the Transition Metals," Academic Press, London (1976).

13) M. Iwata and Y. Saito, *Acta Crystallogr., Sect. B*, **29**, 822 (1973).

14) S. Kida, J. Fujita, K. Nakamoto, and R. Tsuchida, *Bull. Chem. Soc. Jpn.*, **31**, 79 (1958).

15) B. Roos, A. Veillard, and G. Vinot, *Theoret. Chim. Acta*, **20**, 1 (1971).

16) T. H. Dunning, Jr., *J. Chem. Phys.*, **53**, 2823 (1970).

17) H. Kashiwagi, T. Takada, E. Miyoshi, and S. Obara, "Program JAMOL2," Program Library, Hokkaido University Computing Center.

18) H. Kashiwagi, *Int. J. Quantum Chem.*, **10**, 135 (1976).

19) H. Kashiwagi and F. Sasaki, *Int. J. Quantum Chem.*, **S7**, 545 (1973).

20) C. C. J. Roothaan, *Rev. Mod. Phys.*, **32**, 179 (1960).

21) H. Kamimura, S. Sugano, and Y. Tanabe, "Ligand Field Theory and Its Applications," 4th ed, Shokabo, Tokyo (1975).

22) M. Sano and E. Miyoshi, Program Library, Institute for Molecular Science Computing Center.

23) M. Sano, Y. Hatano, and H. Yamatera, *Chem. Phys. Lett.*, **60**, 257 (1979).

24) M. Sano, Y. Hatano, and H. Yamatera, *Chem. Lett.*, **1979**, 789.

25) Reference may also be made to a paper to be published in *Bull. Chem. Soc. Jpn.*, **54** (M. Sano, H. Adachi, and H. Yamatera) in which the results of discrete variational Xα calculations are described on $[Co(CN)_6]^{3-}$ and other hexacyano complexes, together with the free cyanide ion.

26) Wave-function contours are here preferred to the numerical orbital populations given in Ref. 23, since the latter may be artifacts to some extent (Ref. 24). See also Ref. 25.

27) S. Inagaki and K. Fukui, *Chem. Lett.*, **1974**, 509.

28) S. Inagaki, H. Fujimoto, and K. Fukui, *J. Am. Chem. Soc.*, **98**, 4054 (1976).

29) T. Koopmans, *Physica*, **1**, 104 (1933).

30) A. Veillard and J. Demuynck, "Application of Electronic Structure Theory," ed by H. F. Schaefer, III, Plenum Press, New York (1977), p. 187.

31) The situation is analogous to the case of the oxide ion; the O^{2-} ion is stable in the crystals of metal oxides in spite of the fact that reaction, $O^{2-} \rightarrow O^- + e$, is exothermic, or that the ionization potential of O^{2-} is negative.

32) H. Johansen and U. Wahlgren, *Mol. Phys.*, **33**, 651 (1977).

33) C. K. Jørgensen, *Adv. Chem. Phys.*, **5**, 33 (1963).